Influence of the plate leading-edge shape and thickness on the boundary layer laminar-turbulent transition at Mach number M=5

Sergey V. Aleksandrov[1], Eugenia A. Aleksandrova[2], Volf Ya. Borovoy[3], Vladimir E. Mosharov[4], Vladimir N. Radchenko[5] and Alexander V. Fedorov [6]

Central Aerohydrodynamic Institute (TsAGI)

Zhukovsky Str. 1, Zhukovsky, Moscow region 140180, Russia,

[1] *splavgm@gmail.com;* [2] *miptjane@gmail.com;* [3] *volf.borovoy@gmail.com;* [4] *mosh@progtech.ru;* [5] *vradchenko61@gmail.com;* [6] *fedorov@falt.ru*

Abstract

The results of experimental study of boundary layer laminar-turbulent transition on a blunted plate with leading edges of various shapes and thicknesses at free-stream Mach number M_∞=5 and unit Reynolds numbers Re_1 from 1.5×10^7 to 9×10^7 m^{-1} are presented. The Reynolds number Re_b, calculated by leading edge thickness b, was varied from 0 to 2×10^6. The following leading edge shapes were studied: cylinder, flat face, ellipse, and "smoothed cylinder". They were chosen by the results of numerical study of a non-viscous gas flow around a blunted plate. It was shown that at $Re_b<0.5\times10^5$, the shape of the leading edge practically does not affect the transition position. At the same time, the laminar flow segment is monotonously extended as b increases. For large Re_b values the variation of leading edge shape significantly changes the transition position. A laminar – turbulent transition reversal was observed for all investigated shapes of leading edge. However, the Reynolds number Re_b, at which the reversal occurs, depends significantly on the edge shape. The possibility of laminar flow segment extension by reasonable selection of blunting shape and thickness is shown.

1. Introduction

Laminar-turbulent transition of the boundary layer at supersonic speeds is one of the fundamental scientific problems of modern aerodynamics. This problem is also of great practical importance: the delaying of transition zone from the fuselage nose and the wing leading edge reduces the drag, the heat flux, and the weight of required heat shield. On the other hand, the turbulization of boundary layer in front of the air intake can significantly improve its characteristics.

Many investigations have been devoted to the transition problem (see, for example, [1–7]). The experiments were carried out both in ground facilities and in real flight conditions. Most studies are devoted to investigation of the transition on simple-shape bodies: a cone simulating the fuselage, and a plate simulating the wing and the tail of the aircraft.

The fuselage and the wing of hypersonic aircraft are usually blunted that is necessary to decrease the structure heating. Experiments [1], carried out more than 50 years ago, have shown that the blunting moves the zone of laminar-turbulent transition downstream and significantly extends the segment of laminar flow. This is caused by the drop of total pressure behind the bow shock wave generated by blunting, and, as a consequence, by the decrease of local Reynolds number. However, the elongation of the laminar segment occurs only to a certain critical thickness of blunting. Exceeding this value causes the opposite effect, called the reversal of laminar-turbulent transition: the transition zone begins to move back to the nose and at sufficiently large bluntness thicknesses the transition occurs on the nose. A detailed analysis of the experimental data demonstrating this effect was made in [2]. The studies were continued in experiments [3-6] conducted on cones with spherically blunted noses at Mach numbers from 6 to 10 in a wide range of Reynolds numbers.

The transition reversal was also observed in experiments on blunted plates. An overview of the data describing the effect of plate blunting on transition position at supersonic and hypersonic flow speeds is given in [4]. In TsAGI, the transition reversal on a flat plate with a cylindrical leading edge was also revealed at flow Mach number M_∞=5 [7, 8].

S.V. Aleksandrov, E. A. Aleksandrova, V.Ya. Borovoy, V. E. Mosharov, V. N. Radchenko, A.V. Fedorov

A number of theoretical studies [9–11] are devoted to transition reversal, but so far this phenomenon is not explained.

In previous works devoted to the influence of blunting on laminar-turbulent transition, the effect of the leading edge shape was not studied. The only known exception is the work [2] in which an attempt was made to shift back the transition on the cone by reducing the pressure gradient downstream of the spherical nose. However, this led to the opposite result due to a significant pressure increase behind the nose. Perhaps this problem did not attract attention because the transition was studied mainly at a large relative distance from the cone nose and the plate leading edge (at $X/b \sim 100$ or more). However, as this study has shown, the shape of blunting can significantly affect the laminar-turbulent transition also at large distances from the nose. This occurs, primarily, because the distancing of bow shock wave and its shape, and, consequently, the thickness of the High-Entropy Layer (HEL), depend on the shape of blunting. In addition, the blunting shape significantly affects the magnitude of maximal pressure gradient in the zone of junction of blunting with a conical or flat surface.

This work is devoted to the study of the flow around a plate with blunting of various shapes. It is shown that by changing the profile of plate leading edge, it is possible to control the position of laminar-turbulent transition: to move the transition zone downstream from the leading edge or upstream.

2. Calculation of the flow around a blunted plate and the choice of the shape of experimental models

To obtain preliminary information on the influence of the leading edge shape on the flow around the plate and to choose the model geometry reasonably, a numerical study of the flow around the blunted plate by an inviscid gas was carried out.

The calculations were performed using the HSFlow software package [12] for an inviscid perfect gas with a ratio of specific heats γ=1.4 and a Prandtl number Pr=0.72. The scheme of the computational domain is shown in Figure 1. A no-flow condition was specified on the body contour (line 1). Rankine-Hugoniot relations were fulfilled on the bow shock wave (line 2), the extrapolation condition was satisfied at the end of the computational domain (line 3), and the condition of flow symmetry – on the abscissa axis. A block-structured computational mesh with the number of nodes 668×250, thickened near the body surface, was used. The mesh was adapted to the shape of the bow shock wave shape to reduce the "noise" of the shock wave. This trick significantly reduced disturbances both on the shock wave and behind it, and increased the accuracy of pressure distribution calculation.
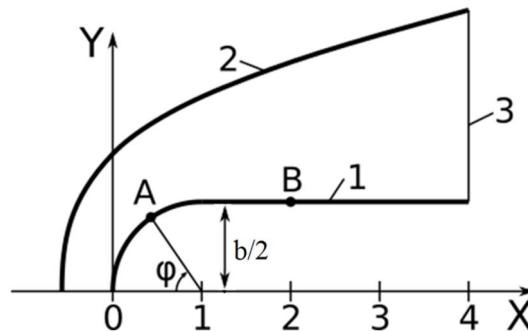
Figure 1: Scheme of the computational domain

The flow around a flat plate with two leading edge profiles was calculated (the linear dimensions are related to the half-thickness of the leading edge $b/2$):

1) elliptical profiles with different values of the axes ratio $e=a/b$, where a is the length of the axis parallel to the plate surface, and b is the length of the lateral axis. The ratio of the axes was varied from e=0 (flat face) to e=2.0 (elliptical nose).

2) "smoothed cylindrical" profile: from the frontal point (X=0, Y=0, φ=0, Fig. 1) to point A with coordinates X=0.25, Y=0.66, φ=41.4°, the profile coincides with the cylinder (point A is located in front of the sound point, the coordinates of which are X=0.31, Y=0.72, φ=46.4°). From point A to the point of junction with a flat surface B, the profile is described by 4 polynomials of the 3rd order, conjugated to each other without breaking the second derivative.

The investigation of the flow around the second profile allows answering the question of whether the local changes of the blunting shape and the pressure gradient affect the transition position. The choice of a profile of the second type is based on the next reasons. An elliptical profile is elongated in the direction of the free stream and at sufficiently large value of e (e.g. e=2) provides smooth junction of the blunting with a flat surface and, as a result, a small positive pressure gradient at the junction point. However, the curvature radius near the frontal point is reduced

DOI: 10.13009/EUCASS2019-384

Influence of the plate leading-edge shape and thickness on the boundary layer laminar-turbulent transition at Mach number M=5

that leads to heat transfer increase in this zone. The profile of the second type provides smooth junction of blunting with a flat surface, keeping the curvature radius in the frontal area and, therefore, does not change the heat transfer level in this area.

The calculations showed that the HEL thickness decreases with an increase of e value. However, at the same time, the pressure change Δp decreases in the zone of junction of blunting with the flat surface, which should favorably affect the laminar-turbulent transition. Numerical calculation does not show a pressure jump at $e \geq 1$, but demonstrates a decrease of pressure gradient in the vicinity of junction point. According to calculations the pressure gradient is zero at $e \geq 1.5$, as well as in the case of a smoothed cylindrical profile.

A zone of increased pressure is formed near the blunted leading edge of the plate, where the pressure distribution strongly depends on the shape of the blunting (Fig. 2). At a small relative distance from the leading edge ($X/b \approx 1.4$), the pressure for all studied leading edge shapes almost coincides, but remains significantly (2.5 times) higher than free stream pressure. In the case of a cylindrical edge, the pressure on the plate is 10% higher than static pressure $p\infty$ even at a distance $X/b=31$. In the book [13], the pressure distribution on the blunted plate at hypersonic speeds is presented as $\Delta p / p_\infty = f(\frac{X}{b} \frac{1}{C_x M^3})$, where Δp is the pressure increment to freestream pressure, C_x is the drag coefficient of the leading edge. This equation means that, in the case of cylindrical blunting, the relative length of increased pressure zone (where $\Delta p / p_\infty \geq 0.1$) at $M_\infty=6$ increases to $X/b=54$, and at $M_\infty=10$ – to $X/b=248$. Calculation show that this distances increases by approximately 35% in the case of flat face blunting and decrease by 20% in the case of elliptical blunting ($e=2$).
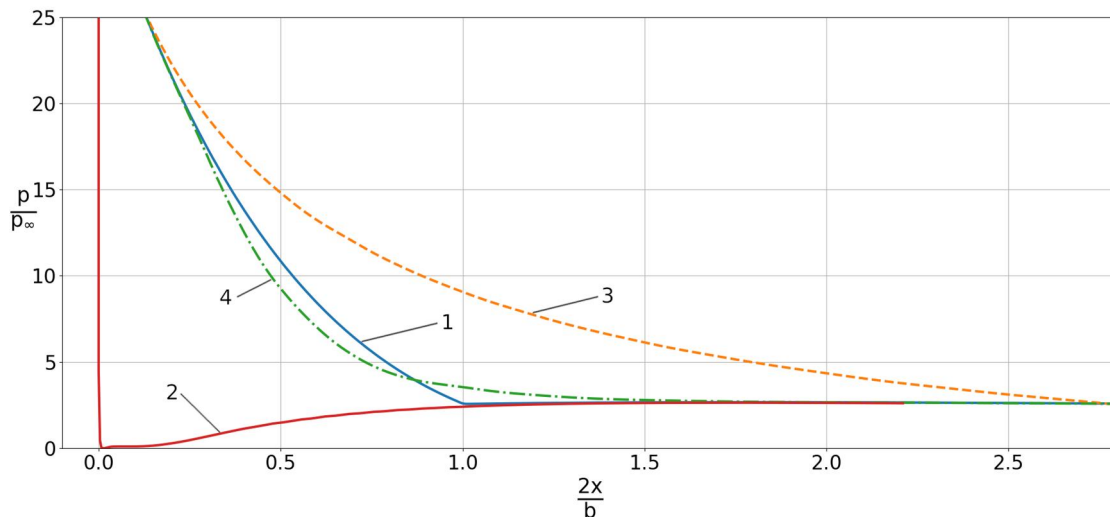
Figure 2: Pressure distribution on the front part of the blunted plate: 1 – cylindrical profile, 2 – flat face, 3 – elliptical profile $e=2$, 4 – smoothed cylindrical profile

Based on the above data, the following four profiles were selected for experimental studies (Fig. 3): flat face with $e=0$, cylinder with $e=1$, ellipse with $e=2$ and smoothed cylinder.
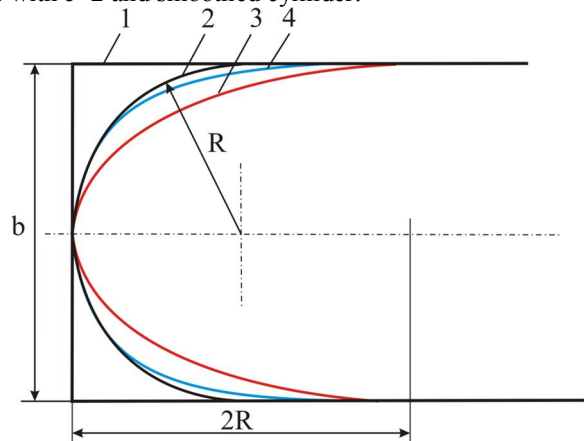
Figure 3: Profiles of investigated edges: 1 – flat face, 2 – cylinder, 3 – ellipse, 4 – smoothed cylinder

S.V. Aleksandrov, E. A. Aleksandrova, V.Ya. Borovoy, V. E. Mosharov, V. N. Radchenko, A.V. Fedorov

3. Experimental models and flow conditions

The main part of the model is steel plate 1 (Fig. 4), to which the interchangeable leading edge 2 is attached. The fences 3are installed on the sides of the plate to prevent gas flowing from the bottom surface of the model to the top. Boundary layer laminar-turbulent transition was studied by measuring the heat flux coefficient distribution. To provide this measurement a thin insert of white opaque plexiglass (4) was glued into the upper surface of steel plate. The second aluminum plate 1 without plastic insert was made to study the flow structure by Schlieren method and by Particle Image Surface Flow Visualization method.
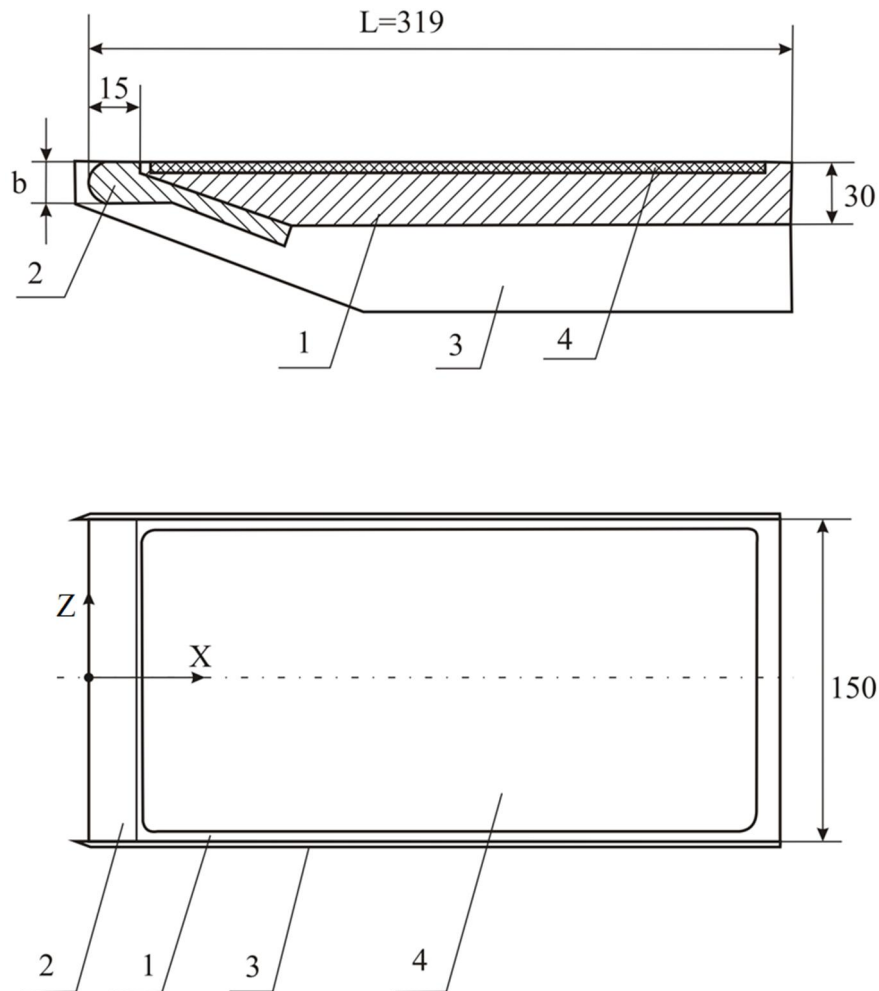
Figure 4: Model layout: 1 – plate, 2 – interchangeable leading edge, 3 – side fences, 4 – plexiglass insert

Edges were made of steel by electro-erosion method. The surface roughness after manufacturing was about 20 micrometers. Then all the edges were manually polished with fine sandpaper to a gloss value. The surface roughness measured after polishing was about 1 micrometer. The thickness of "sharp" leading edge was measured to be about 20 μm. Real dimensions of the edges bluntness were measured accurately using laser probe "FARO Laser Line Probe V3".

26 edges of the next thicknesses b were made: "sharp" – 0.02 mm; cylindrical – 0.3, 0.48, 0.66, 0.76, 1.2, 1.6, 1.78, 2.4, 3.96, 8.0, 19.96 mm; flat faces – 0.2, 0.33, 0.53, 0.7, 0.82, 19.9 mm; elliptical – 1.68, 3.59, 8, 19.78 mm; smoothed cylindrical – 2.0, 3.82, 8.0, 19.7 mm.

The experiments were carried out in a Ludwig-type wind tunnel UT-1M (TsAGI) at Mach number $M_\infty = 5$. A profiled nozzle with an output diameter of 300 mm was used. The duration of steady flow is 40 ms. Each edge was tested at several unit Reynolds number values in the range from $Re_1 \approx 1.5 \times 10^7$ to $Re_1 \approx 9 \times 10^7$ m^{-1}. The stagnation temperature remained approximately constant: $T_0 = 460$–475 K. The temperature factor varied insignificantly: $T_w/T_0 = 0.61$–0.63.

4. Methodology of laminar-turbulent transition research

The state of the boundary layer was determined based on the measurements of heat flux to the model surface q_w. For this purpose, a luminescent Temperature Sensitive Paint was used [14]. As a result of measurements the Stanton number was calculated – the dimensionless heat transfer coefficient:

$$St = \frac{q_w}{c_p U_\infty \rho_\infty (T_0 - T_w)}$$

where: c_p is air specific heat capacity at constant pressure, ρ_∞ and U_∞ are the gas free-stream density and velocity, T_w is the surface temperature and T_0 is the total temperature.

The transition position was determined using a known technique described, for example, in [15]. It is demonstrated below for a flow over the plate with a cylindrical bluntness 0.76 mm thick (see Fig.5).

a)

b)   *c)*
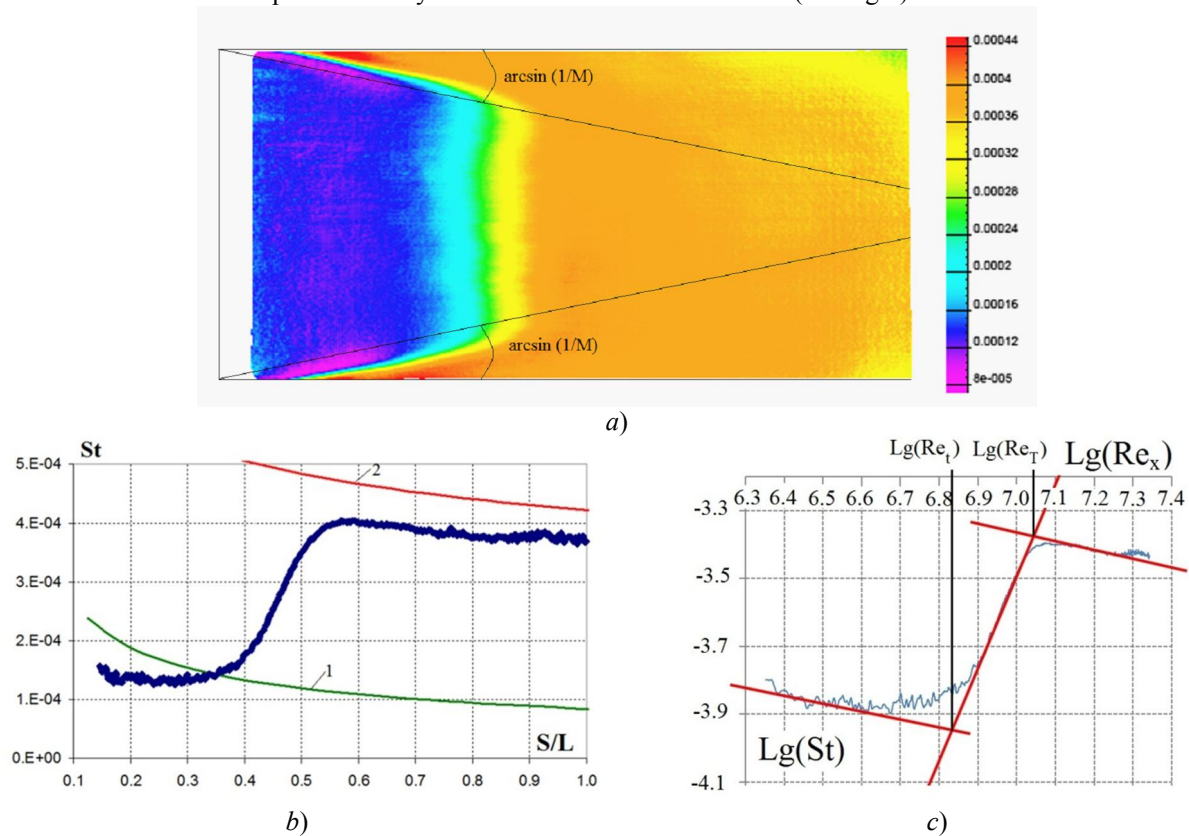
Figure 5: Determination of laminar-turbulent transition position on a plate with a cylindrical bluntness of b=0.76 mm thickness at p_0=48.5 bar, T_0=467 K, $Re_{\infty 1}$=7.5×10⁷, Re_b=5.41×10⁴: *a* – Stanton number distribution on the plate surface; *b* – Stanton number distribution in the central section of the plate, 1 and 2 – calculated values for the laminar and turbulent boundary layer on sharp plate; *c* – Stanton number distribution in logarithmic coordinates

The zone of weak lateral variation of heat flux is highlighted in Figure 5*a*. This zone is bounded by Mach lines emanated from the plate corner points. An inclination angle of these lines at big leading edge thicknesses is significantly larger (up to 30° instead of 20° for the sharp edge) due to the fact that the Mach number in the HEL generated by blunted leading edge is significantly lower than M_∞. Inside the triangle bounded by the leading edge and the lines of plate leading edges influence, the central zone Z=±50 mm was used to determine the state of the boundary layer.

If Z-distribution of heat transfer coefficient was uniform, the transition position was determined in central section Z=0 or near it. At uneven distribution, the analysis was carried out in two sections corresponding to the minimum and maximum length of the laminar zone in the band -50<Z<50 mm. The dependences St=f(X) in selected sections were plotted in natural and logarithmic coordinates, as shown in Figures 5*b* and 5*c*. The onset and end of transition were determined as the coordinates of the points of approximation lines intersections (points S_t and S_T, Fig.5*c*).

5. The results of laminar – turbulent transition investigation

5.1 Cylindrical leading edge

Experimental data on transition position on a plate with cylindrical leading edge are presented in Figure 6. Here $Re_b=\rho_\infty U_\infty b/\mu_\infty$, $Re_t=\rho_\infty U_\infty S_t/\mu_\infty$, $Re_T=\rho_\infty U_\infty S_T/\mu_\infty$, S_t and S_T are the distances along the model contour from the frontal point (lying on the blunting symmetry line) to the onset and end of the transition zone, respectively. The relative distances $S_t/b=Re_t/Re_b$ and $S_T/b=Re_T/Re_b$ are also shown. The presented results (M_∞=5) are in satisfactory agreement with the results obtained by other authors under various conditions both in UT-1M wind tunnel and in a number of other aerodynamic facilities (Fig.7; for UT-1M tunnel – also previously unpublished data of 2010 year).

a)   *b*)
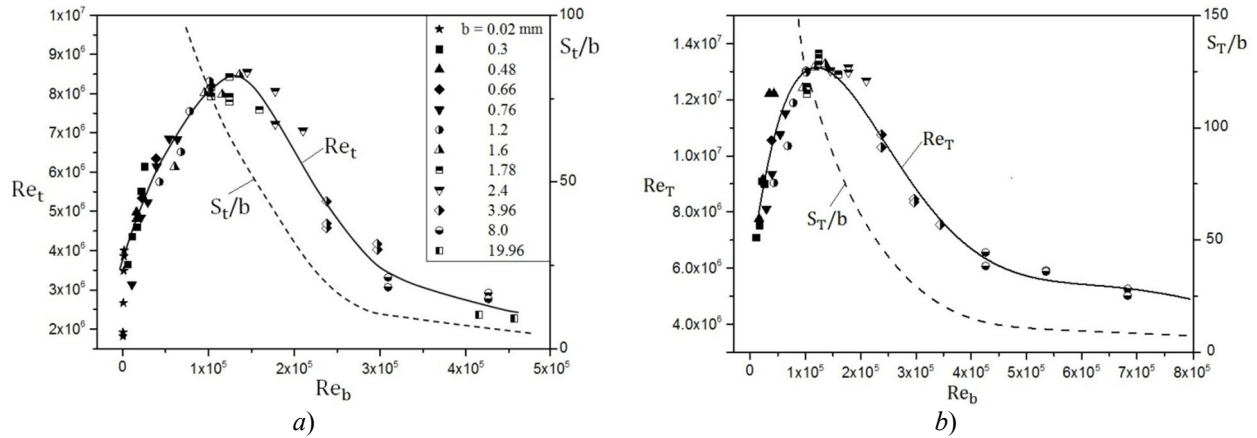
Figure 6: Transition zone position on a plate with cylindrical leading edge: *a* –transition onset, *b* –transition end
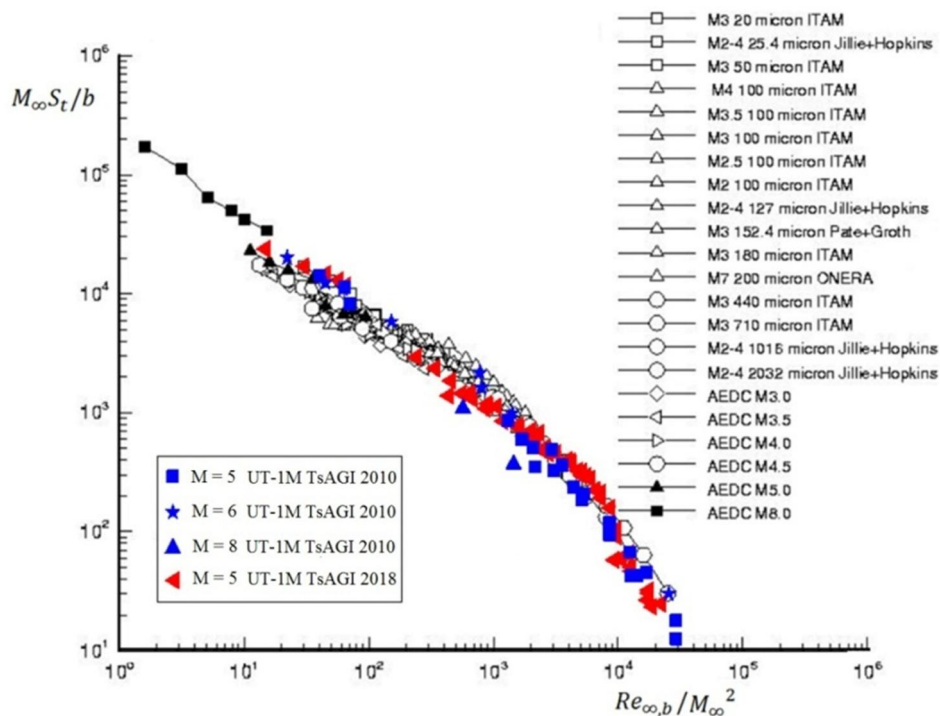
Figure 7: Comparison of experimental results of transition onset on a plate with a cylindrical leading edge obtained in this work with the results of previous studies by TsAGI [7] and the database of work [4]

Figure 6 shows that at Re_b increase from 0 to $\sim 1.5 \times 10^5$ the transition zone moves downstream from the leading edge. This phenomenon is associated with the formation of a High-Entropy Layer behind the bow shock wave, the thickness of which is proportional to the leading edge thickness. The HEL is characterized by a lower density and

higher gas viscosity that leads to a decrease of the local Reynolds number. At $Re_b>1.5\times10^5$ the transition zone moves upstream, that means the transition reversal.

The possible causes of the reversal can be:

1) With the distance increase from the leading edge, the HEL is mixed with the boundary layer and at some distance S_{sw} is completely "swallowed" by the latter. The HEL thickness and its length to the swallowing point increase with leading edge thickening approximately proportionally to b, i.e. faster than laminar segment length S_t. Estimations of High-Entropy Layer and boundary layer thicknesses show that at some Reynolds number $Re_b<10^5$, the HEL is swallowed by the boundary layer at a distance S_{sw}/b lower than the distance to the transition onset point S_t/b. As a result, at sufficiently large leading edge thickness the swallowing point S_{sw} "ovetake" the point S_t. Further HEL thickening does not change the characteristics at external edge of boundary layer, and the elongation of the laminar segment stops. But it must be admitted that this effect can only stabilized the transition position. To explain the transition reversal, some additional mechanism of transition stimulation should be added.

2) During experiments in a wind tunnel, the laminar-turbulent transition is significantly affected by background disturbances presented in the free stream. Studies [16] showed that after passing through a shock wave, the amplitude of the pressure pulsations increases proportionally to the average pressure. This is a consequence of quasi-stationary nature of disturbed flow. Pressure pulsations are amplified passing the bow shock wave, propagate along the characteristic lines and come not only to the frontal surface, but also to the flat plate surface behind the blunting. With an increase of leading edge thickness, the zone of intense pulsations approaches the zone of laminar-turbulent transition, which can cause the reverse movement of transition to the plate leading edge.

3) The measurements show that the relative length of laminar segment S_t/b decreases at an increase of Re_b (Fig.6). On the other hand, the relative length of the high-pressure zone, according to calculations of inviscid flow, does not depend on Re_b. At $M_\infty=5$ the relative length of the zone, where $p/p_\infty\geq1.1$, is $S_p/b=31.3$. Relative length of laminar segment is $S_t/b=130$ at $Re_b\approx0.5\times10^5$, and $S_t/b=53$ at $Re_b\approx1.5\times10^5$, that means that high-pressure zone begins to occupy the bigger part of laminar segment at an increase of Re_b. An increase of relative length of the high-pressure zone S_p/S_t and a corresponding increase of local Reynolds number values may be one of the reasons of Re_t decrease and of transition reversal.

4) Due to the concave shape of streamlines near the stagnation point, the Görtler vortices may appear near the frontal surface of the blunted plate. They can be spread from the blunting to a flat surface and can affect the laminar-turbulent transition. In some experiments of this work, the periodic structures were observed on the plate surface, which, apparently, may be caused by Görtler vortices. However, the well-defined relation of such structures formation and laminar-turbulent transition was not established.

5) Experiments on spherically blunted cones [2] showed that the reversal of laminar-turbulent transition and the transition position after reversal are very sensitive to the details of the flow around the blunted nose. In particular, the results of [2, 17, 18] led to the assumption that the nose roughness on subsonic part of the flow is one of the main sources of the reversal. This assumption is confirmed in [19], where a review of the results of modern experimental studies of the combined effect of blunting and roughness on blunted cones, as well as the results of a theoretical analysis of transient growth of disturbances induced by roughness is given. Probably, the similar effects are realized also in the flows over the blunted plates.

The laminar-turbulent transition and the transition reversal can also be affected by local features of leading edge shape, which change the pressure gradient in the zone of the leading edge juncture with a flat surface, or cause separation of boundary layer. These effects are discussed below.

It should be noted that the transition reversal occurs at large distances from the blunted nose (as a rule, $S_t/b\sim100$). Because of restricted model length, the reversal can be observed at relatively small bluntness thicknesses and large unit Reynolds numbers. However, in these cases it is difficult to control, select and explore various processes occurring in the flow around the miniature nose parts. Similar difficulties arise in direct numerical simulation, since it is necessary to resolve small-scale perturbations on blunting and to calculate with high accuracy the development of these perturbations over long distances downstream. Therefore, the physical nature of the reversal is still not clear; i.e. it is not clear which of the mentioned above mechanisms and under what conditions has the main influence.

5.2 Flat face and cylindrical leading edges

Comparison of data for flat face and cylindrical leading edges is interesting because they differ principally from each other: a flat face profile, unlike a cylindrical one, has an angular point, which causes boundary layer separation at sufficiently large Reynolds numbers.

S.V. Aleksandrov, E. A. Aleksandrova, V.Ya. Borovoy, V. E. Mosharov, V. N. Radchenko, A.V. Fedorov
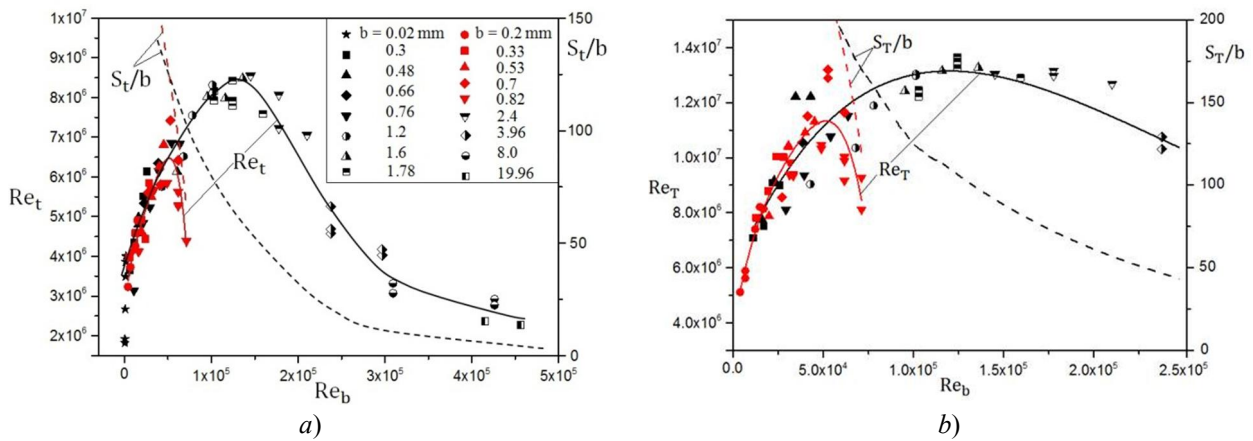
Figure 8: Laminar-turbulent transition on a plate with flat face edge (red symbols) and with cylindrical edge (black symbols): a –transition onset, b –transition end

Comparison of the Reynolds numbers Re_t and Re_T for these shapes (Fig.8) shows that at $Re_b \leq 0.5 \times 10^5$ even such a dramatic change of leading edge shape has practically no effect on the transition. This is a result of the influence of gas viscosity on the flow around the leading edge.

The transition reversal on a flat-faced plate occurs at the Reynolds number, which practically coincides with the mentioned above limit of nose shape influence on the transition ($Re_b \approx 0.5 \times 10^5$). On a plate with a cylindrical blunting, the reversal occurs at significantly higher Reynolds number $Re_b \approx 1.5 \times 10^5$. It should be noted that at the same leading edge thickness, the HEL thickness is 1.66 times bigger in the case of flat-faces blunting than in the case of cylindrical one. However, even taking into account this factor, the effective value of Re_b of transition reversal beginning at flat face blunting ($Re_b \approx 0.83 \times 10^5$) is significantly lower than in the case of cylindrical blunting. It is also important that exceeding the critical Re_b value in the case of flat face blunting leads to a faster forward movement of laminar-turbulent transition in respect with cylindrical blunting. Thus, in quite wide range of $Re_b = 0.8 \times 10^5 - 3 \times 10^5$, the replacement of cylindrical blunting with a flat face leads to a sharp decrease of the laminar segment. Therefore, flat face blunting can be used as transition stimulator.

The transition reversal behind flat face occurs at large distance of transition point from leading edge ($S_t/b = 125$, Fig.8a) and is not caused by pressure pulsations in free stream and by lengthening of high pressure zone. The cause of this difference is that a well-developed separation zone is formed on a flat face plate at quite large Reynolds numbers. This is demonstrated by Schlieren photos (Fig.9), as well as by surface flow visualization on the plate with viscous oil. In contrast, flow separation was not found on the plate with a cylindrical blunting.
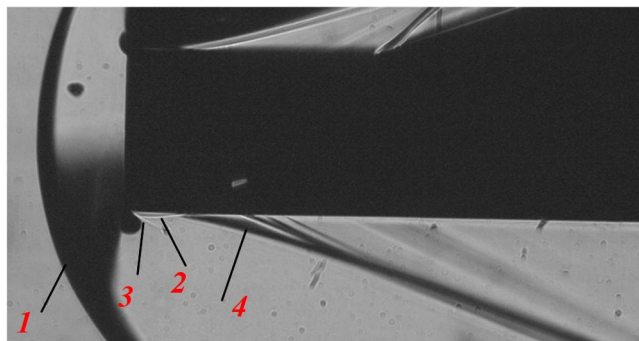
Figure 9: Schlieren photo of the flow around a flat face plate at $Re_b = 8.4 \times 10^5$:
1 – bow shock wave, 2 – separation zone, 3 – separation shock, 4 – reattachment shock

Figure 10 shows the distribution of the Stanton number on the plate surface for two values of the Re_b number: $Re_b = 2.8 \times 10^4$ which is lower than the critical value $Re_b \approx 5 \times 10^4$ corresponding to the transition reversal beginning, and $Re_b = 7.13 \times 10^4$ – which is bigger. Prior to the beginning of the reverse (Fig.10a), the lines of constant St number have the form of straight lines parallel to the plate leading edge. This also concerns the laminar-turbulent transition line. In the second case (Fig.10b) these lines have a wavy shape that is probably caused by boundary layer separation. Longitudinal vortices can be generated near reattachment line, which cause non-uniform lateral heat transfer distribution. Such non-uniformity begins to appear on a plate with flat face blunting $b = 0.7$ mm at $Re_b \approx 0.62 \times 10^4$, which approximately corresponds to the transition reversal.

a)

b)
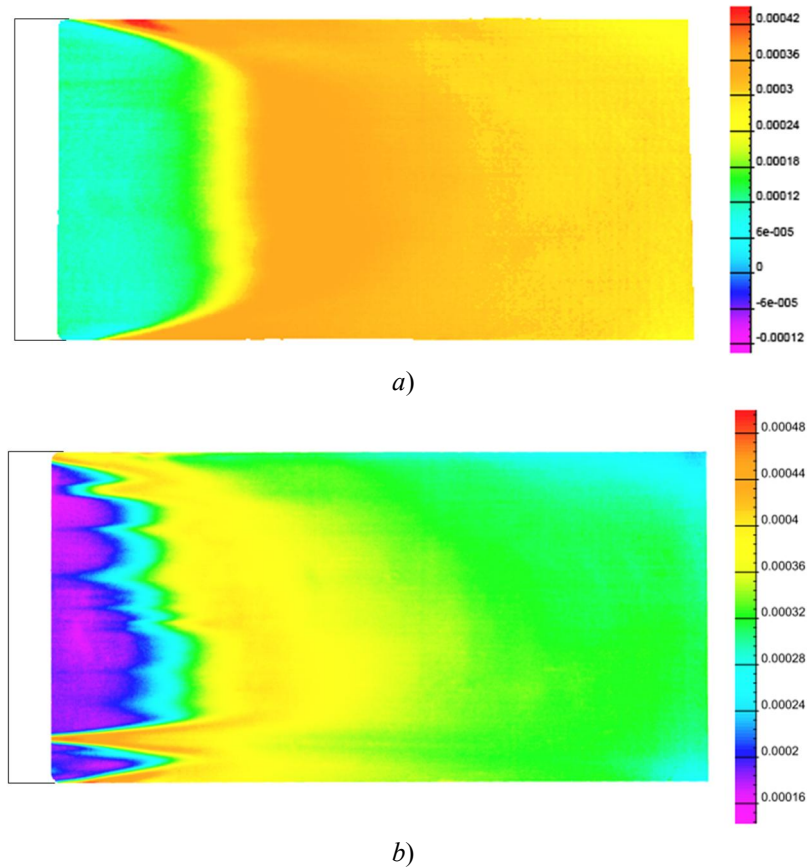
Figure 10: Stanton number Distributions on the plate surface with flat face blunting:
$a - b$=0.33 mm, Re_b=2.8×10^4, $b - b$=0.82 mm, Re_b=7.13×10^4

a)   *b*)
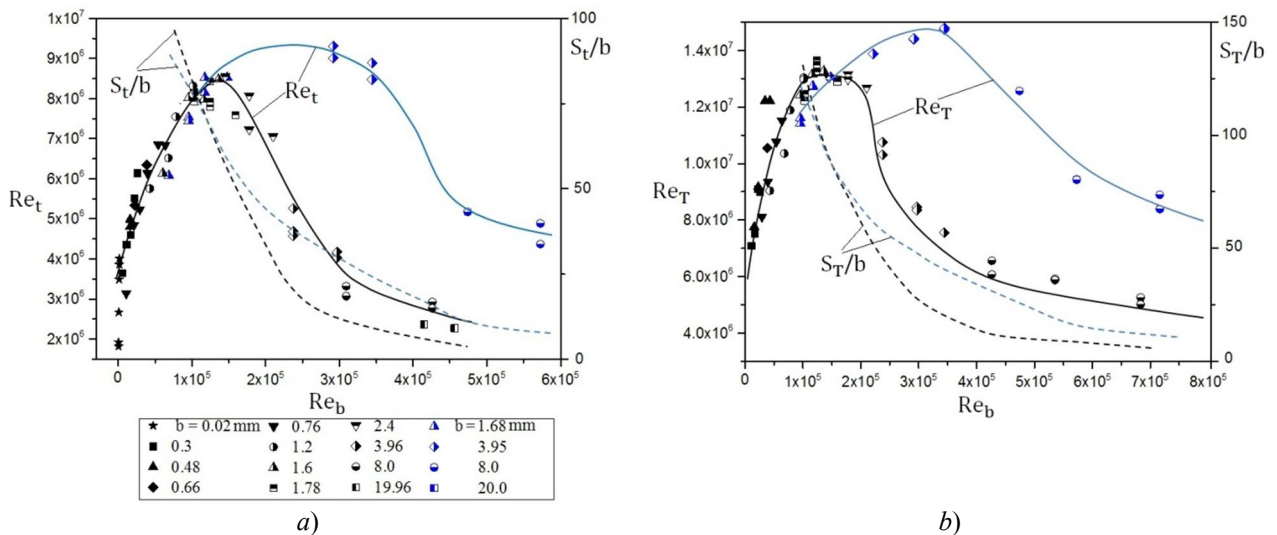
Figure 11: Laminar-turbulent transition on a plate with elliptical (blue symbols) and cylindrical (black symbols) leading edges: *a* – transition onset, *b* – transition end

5.3 Elliptical and cylindrical leading edges

Comparison of data for elliptical and cylindrical leading edges (Fig. 11) shows that the Reynolds number Re_b, at which the transition reversal begins, is approximately 2 times greater in the first case than in the second. The

S.V. Aleksandrov, E. A. Aleksandrova, V.Ya. Borovoy, V. E. Mosharov, V. N. Radchenko, A.V. Fedorov

advantage of an elliptical edge is retained notwithstanding the fact that high-entropy layer on elliptical edge is 1.6 times thinner than on cylindrical one.

The reason for later reversal beginning on the plate with elliptical edge in comparison with cylindrical edge is the smoother shape of first profile. Although some small discontinuity of curvature remains in the point of junction of elliptical edge with the plane, the pressure gradient at this point is much smaller than in the case of a cylindrical edge (in numerical calculation it was obtained to be zero, see Fig.2).

From Figure 11 it follows that in a wide range of Reynolds numbers $Re_b=2\times10^5$–6×10^5 the replacement of cylindrical shape with an elliptical one allows to lengthen significantly the laminar part of the flow.

5.4 Smoothed and cylindrical leading edges

Difference of smoothed cylindrical profile in respect with the cylindrical one is that the contour between the sound point and the point of junction with the plate is elongated and the junction is made without breaking the curvature. As a result, the normalized pressure gradient in the junction zone is reduced (according to the calculation, from $dp/dS=0.0086$ to $dp/dS=0$, Fig.2). The data presented in Fig. 12 show that at Reynolds numbers $Re_b\leq3\times10^5$, the profile smoothing does not affect the position of the transition zone. However, at large Reynolds numbers the transition zone is systematically shifted 15-30% downstream due to the smoothing of the profile.
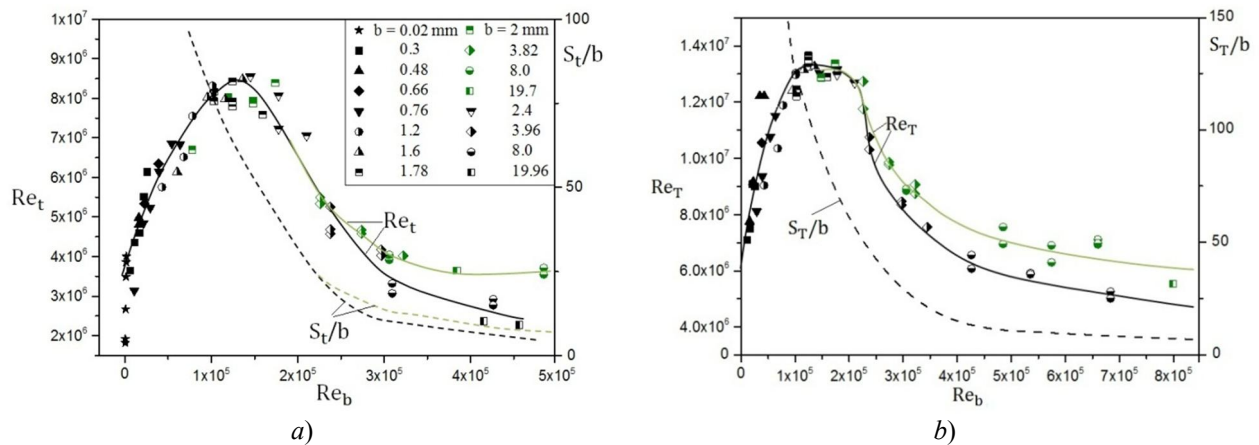
Figure 12: Laminar-turbulent transition on a plate with smoothed (green symbols) and cylindrical (black symbols) leading edges: *a* – transition onset, *b* – transition end

Conclusion

The study showed that at small values of Reynolds number Re_b calculated by plate leading edge thickness b (in the range $Re_b<0.5\times10^5$ at $M_\infty=5$), the shape of the leading edge practically does not affect the position of laminar-turbulent transition because of large viscosity effects on the flow around the edge.

At larger Re_b values, the variations of leading edge shape led to a significant change in transition position. The laminar segment on flat-face blunted plate at $Re_b>0.8\times10^5$ is much shorter than on cylindrical one, and on elliptically blunted plate at $Re_b>2\times10^5$ – much longer than on cylindrical one. A local change of leading edge shape (profile smoothing) extends a little the transition zone at large Re_b values.

The existence of laminar-turbulent transition reversal on cylindrically blunted plate was confirmed. The investigated shapes of leading edge did not eliminate the reversal. However, it was established that replacing of cylindrical blunting with elliptical one significantly increases the critical Reynolds number value Re_b, at which the reversal begins, and also reduces the rate of laminar segment contraction when this critical value is exceeded. In contrast, the replacement of a cylindrical blunting with a flat face significantly reduces the critical value of Re_b and accelerates the contraction of the laminar segment at supercritical values of Re_b.

Thus, it is shown that variation of leading edge shape and thickness allows to lengthen or shorten the laminar segment of the flow around the plate.

Acknowledgments

DOI: 10.13009/EUCASS2019-384

Influence of the plate leading-edge shape and thickness on the boundary layer laminar-turbulent transition at Mach number M=5

References

[1] Stetson K.F., Rushton G.H. 1967. Shock tunnel investigation of boundary-layer transition at M=5.5. *AIAA J.* 5(5): 899-906.

[2] Stetson K.F. 1983. Nosetip bluntness effects on cone frustum boundary layer transition in hypersonic flow. *AIAA*-83-1763.

[3] Maslov A.A. 2001. Experimental study of stability and transition of hypersonic boundary layer around blunted cone. *Technical report, Institute of Theoretical and Applied Mechanics, Russian Academy of Sciences.*

[4] Simeonides G.A. 2003. Correlation of laminar-turbulent transition data over flat plates in supersonic/hypersonic flow including leading edge bluntness effects. *Shock Waves.* 12: 497-508.

[5] Brazhko V.N., Vaganov A.V., Kovaleva N.A., Kolina N.P., Lipatov I.I. 2009. Experimental and numerical investigations of boundary layer transition on blunted cones at supersonic flow. *TsAGI Science Journal.* 40(3): 309-319.

[6] Aleksandrova E.A., Novikov A.V., Utyuzhnikov S.V., Fedorov A.V. 2014. Experimental study of the laminar-turbulent transition on a blunt cone. *Journal of Applied Mechanics and Technical Physics.* 55(3): 375-385.

[7] Novikov A.V., Pesetskaya E.A., Skuratov A.S. 2011. Experimental study of laminar-turbulent transition on a flat blunt plate. In: *XV International Symposium in Methods of discrete singularities in problems of mathematical physics*, (in Russian).

[8] Borovoy V.Ya., Mosharov V.E., Radchenko V.N., Skuratov A.S. 2018. Shock wave interaction near a cylinder aligned normal to a blunted plate – Part I: Gas flow and heat transfer on a plate near a cylinder. *TsAGI Science Journal.* 49(2): 105–118.

[9] Zhong X., Wang X. 2012. Direct numerical simulation on the receptivity, instability, and transition of hypersonic boundary layers. *Annu. Rev. Fluid Mech.* 44: 527–561.

[10] Fedorov A.V. 1990. Instability of the entropy layer on a blunt plate in supersonic gas flow. *Journal of Applied Mechanics and Technical Physics.* 5: 63-69 (in Russian).

[11] Paredes P., Choudhari M.M., Li F., Jewell J.S., Kimmel R.L., Marineau E.C., Grossir G. 2018. Nosetip bluntness effect on transition in hypersonic speeds: experimental and numerical analysis under NATO STO AVT-240. *AIAA*-2018-0057.

[12] Egorov I.V., Novikov A.V. 2016. Direct numerical simulation of laminar–turbulent flow over a flat plate at hypersonic flow speeds. *Computational Mathematics and Mathematical Physics.* 56(6): 1048–1064. doi: 10.7868/S0044466916060120

[13] Cherny G.G. 1956. Gas flows at high supersonic speeds. (in Russian).

[14] Mosharov V.E., Radchenko V.N. 2007. Measurement of heat flux fields in short-duration wind tunnels with Pressure Sensitive Paint. *TsAGI Science Journal.* 38(1-2): 94-101 (in Russian).

[15] Bertin J. Hypersonic Aerothermodynamics. *AIAA Education Series.*

[16] Skuratov A.S., Fedorov A.V. 1991. Characteristics of pressure pulsations in a supersonic wind tunnel and their influence on boundary layer laminar-turbulent transition. *TsAGI Science Journal.* 22(5): 60-68 (in Russian).

[17] Bountin D.A., Gromyko Yu.V., Polivanov P.A., Sidorenko A.A., Maslov A.A. 2016. Effect of roughness of the blunted cone nose-tip on laminar-turbulent transition. In: *International Conference on the Methods of Aerophysical Research (ICMAR 2016), AIP Conf. Proc.* 1770: 030064-1–030064-5. doi: 10.1063/1.4964006.

[18] Zanchetta M.A., Hiller R. 1996. Blunt cone transition at hypersonic speeds: the transition reversal regime. In: *Transitional Boundary Layers in Aeronautics*: 433–440.

[19] Paredes P., Choudhari M.M., Li F., Jewell J.S., Kimmel R.L., Marineau E.C., Grossir G. 2019. Nose-tip bluntness effects on transition at hypersonic speeds. *J. of Spacecraft and Rockets.* 56: 369-387. doi: 10.2514/1.A34277